Effect of Poly Lactic Acid (PLA) Functionalization on Morphological, Electronic and Mechanical Properties of Carbon Nanotubes-A Computational investigation

BY

SALMAN U ZAMAN

NUST00000203266

Supervisor

Dr. Fouzia Malik

MS Computational Sciences and Engineering

(Specialization: Computational Chemistry)

Research Center for Modeling and Simulation

National university of Sciences and Technology

Islamabad, Pakistan

Sep, 2020

Effect of Poly Lactic Acid (PLA) Functionalization on Morphological, Electronic and Mechanical Properties of Carbon Nanotubes-A Computational investigation

BY

SALMAN U ZAMAN

NUST00000203266

Supervisor

Dr. Fouzia Malik

A thesis submitted in the partial fulfillment of the requirements

For the degree of Master of Sciences

In

Computational Sciences & Engineering

RESEARCH CENTER FOR MODELING AND

SIMULATION (RCMS)

NATIONAL UNIVERSITY OF SCIENCES AND

TECHNOLOGY (NUST)

ISLAMABAD, PAKISTAN 2020

Dedicated to . . .

My parents & Brothers

Statement of Originality

I hereby declare that my thesis work titles "Effect of Poly Lactic Acid (PLA) functionalization on Morphological, Electronic and Mechanical Properties of Carbon Nanotubes- A Computational investigation" is carried out by me under the supervision of Dr. Fouzia Malik at Research Center for Modeling and Simulation (RCMS) in National University of Sciences and Technology (NUST). I solemnly declare that to the best of my knowledge, this is my original work and it contains no material which has been accepted for the award of other degree in my name, in any other university. Also no material previously published or written by other person has been included in this except where due reference has been made to the previously published work.

Salman U Zaman

MS Computational Sciences & Engineering

Acknowledgements

I am very thankful to the Almighty Allah for giving good health, strength and opportunity to complete this work. I would like to begin by sincerely thanking my advisor Dr. Fouzia Malik Associate Professor, Research Center for Modeling and Simulation (RCMS), National University of Sciences and Technology (NUST) for her constant support, guidance throughout my course work and research work. She gave me the freedom to define my research and always acted as a very helpful sounding board for my ideas. Whenever I was bereft of ideas, my discussions with her always helped me get back on the right track. She has always encouraged me to pursue more, to full fill dreams and also helped me to explore wonderful moments during research.

I am also very thankful to GEC members – Dr. Rehan Zafar Paracha Assistant Professor, RCMS, NUST and Dr. Rafia Mumtaz Assistant Professor, SEECS, NUST for giving me valuable suggestions, cooperation and support during my research. It would be remiss not to mention the names of Engr. Muhammad Usman, Engr. Muhammad Hassan, Mr. Asim Younas and Mr. Shahzad Khan for their assistance at Super Computing Lab RCMS, NUST. I would like to thank all my teachers at RCMS, Lab fellows for their support during all my stay at RCMS.

On a personal note, I know that this work could not have been completed without the tremendous support of my friends and family. Finally, my gratitude to my parents is beyond measure – all through my life, they have always sacrificed to ensure that I had the best opportunities possible and they have constantly believed in me and encouraged me to dream big and to pursue those dreams. I cannot put into words what their support has meant to me over the years and I dedicate this thesis to them.

TABLE OF CONTENTS

List of Abbreviations

LA	Lactic Acid
PLA	Poly Lactic Acid
SWNT	Single Wall Carbon Nano Tube
MWCN	Multi Wall Carbon Nano Tube
CNT	Carbon Nano Tube
LDA	Local Density Approximation
GGA	Generalized Gradient Approximation
DFT	Density Functional Theory
HOMO	Highest Occupied Molecular Orbital
LUMO	Lowest Unoccupied Molecular Orbital

List of Tables

List of Figures

Abstract:

In new era, much attention have been paid towards nanomaterial due to their greater compatibility, high mechanical and thermal properties. CNTs are among nanomaterials having excellent conductivity, mechanical, and morphological characteristics, however complexity of their production and expensive nature provide an alternative option to produce functional composite. In current research we carried out *in-silico* design of CNTs composite with PLA.PLA is an organic compounds and have ability to adsorb on the surface of CNTs. Ten SWCNT of three different dimensions were selected for the adsorption of PLA on their surface using Density functional theory (DFT/GGA+PW91, Relativity: scaler) along with double zeta basis set, To study the mechanism of adsorption, we determined electronic, kinetic, thermodynamic, and mechanical properties of CNTs before and after adsorption of PLA adsorption..

Highest Kd is observed for 4, 4 CNT/PLA composite *i.e.*, 2.74×10^{20} M^{-1} among armchair CNTs composite, Among chiral composite, 2, 3 CNT exhibited strongest binding with Kd value of $6.4321 \times 10^{8} M^{-1}$ whereas 4, 0 zigzag CNTs furnished binding affinity of 2.6897×10^{21} M^{-1} indicating that 4, 0 zigzag CNTs complex with PLA is of strongest nature, 4, 0 zigzag CNTs respectively owing more adsorption. Enthalpy and Entropy contribution showed the strong binding.

On the basis of HOME - LUMO gap, it indicated that 4, 0 CNT/PLA composite is good conductive among all with electrical conductivity of 39.7×10^{-4}S/m. Young modulus indicated highest mechanical strength for 4, 5 CNT/PLA composite which is 9.94×10^{8} Pa. The current research reveal excellent application of CNT/PLA composite in mechanical industries to lift heavy load with greater elongation and electronics industry with low resistance and high conductivity.

Chapter 1

Introduction

1 Introduction

1.1 Background

Other than precious stone, graphite and C_{60}, the semi one-dimensional nanotube is another type of carbon. Since their revelation in 1991 by Iijima, carbon nanotubes (CNTs) have caught the consideration of scientists around the world.[1] [2] [3] On account of the ideal plane and high characteristic quality of the sp^2—sp^2 covalent holding between carbon particles,[4] CNTs have remarkable mechanical properties[5], indicating high Young's modulus , a high elastic quality, high crack strain and have a very little size, high thermal stability, good electrical[6] [7] , Mechanical, Electrical and optical properties.

Research has concentrated on the reinforcement of CNT strengthened polymers composites, including PMMA and different sorts of epoxy resin, and result in 20-50 % strengthening of CNTs has been accomplished. Moreover numerous scientist made CNT polymer composite yet gain little improvement like its mechanical properties, thermal stability and electrical conductivity[8] [9] [10]. It had been pointed out that composites of CNT of ceramic production are poor for bonding between them.[11] [12] [13]

CNT reinforced Poly Lactic Acid composites is as yet another subject. This chemical method is to made CNT/PLA composite involve adsorption of PLA on the surface of CNT utilizing Density functional theory method (DFT). In present research we revealed morphological properties of CNT/PLA composite to enhanced mechanical properties, electrical conductivity, and its strength.

1.2 Classification of Carbon Nano Tubes (CNTs)

There are two primary kinds of CNTs, (a) single wall carbon nano Tube (SWCNT) (b) multiwall carbon nano tube[14] [15] (MWCNT.)

1.2.1 Single Wall Carbon Nano Tube (SWCNT):

SWNT tubes are characterized as a one dimensional, roundly molded allotropes of carbon that have a high surface region and aspect ratio (length to diameter ratio).The diameter range for SWCNT is up to 0.7 nm and have variable diameter.[16] [17] [18]

SWCNT are further classified into three types, Chiral (n ≠ m), Armchair (n = m) and Zigzag (n, 0)

Chiral CNT: In chiral CNT n ≠ m e.g., (2, 3) and (4, 3) Chiral CNTs possess metallic properties.

Arm chair: For arm chair CNTs n and m identical e.g., (2, 2) and (3, 3). Arm chair carbon Nano have chiral angle of 30^0 and are metallic in nature.

Zigzag: For zigzag m=0 and n is any constant number e.g., (2, 0), (3, 0) etc. Zigzag CNT are used in nano scale sensor. [19]

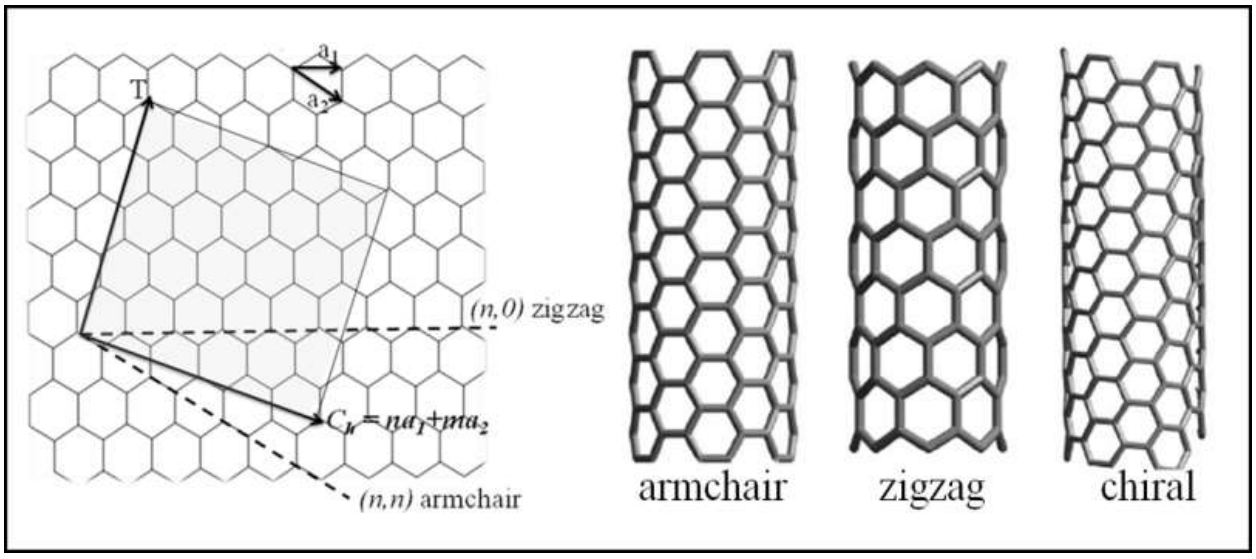

Figure 1.1 Dimension of SWCNTs

1.3 Poly Lactic Acid:

Among wide scope of the bio-polymers accessible, Poly Lactic Acid (PLA) is one of the most generally utilized biodegradable polymers in therapeutic because of its remarkable mechanical properties, minimal effort, great bio-compatibility, and processablity.[20 21 22] PLA is obtained from ring-opening polymerization of lactide, a dimer of lactic acid which is synthesized from fermentation of cornstarch.[23] According to the scheme given below scheme 1.2

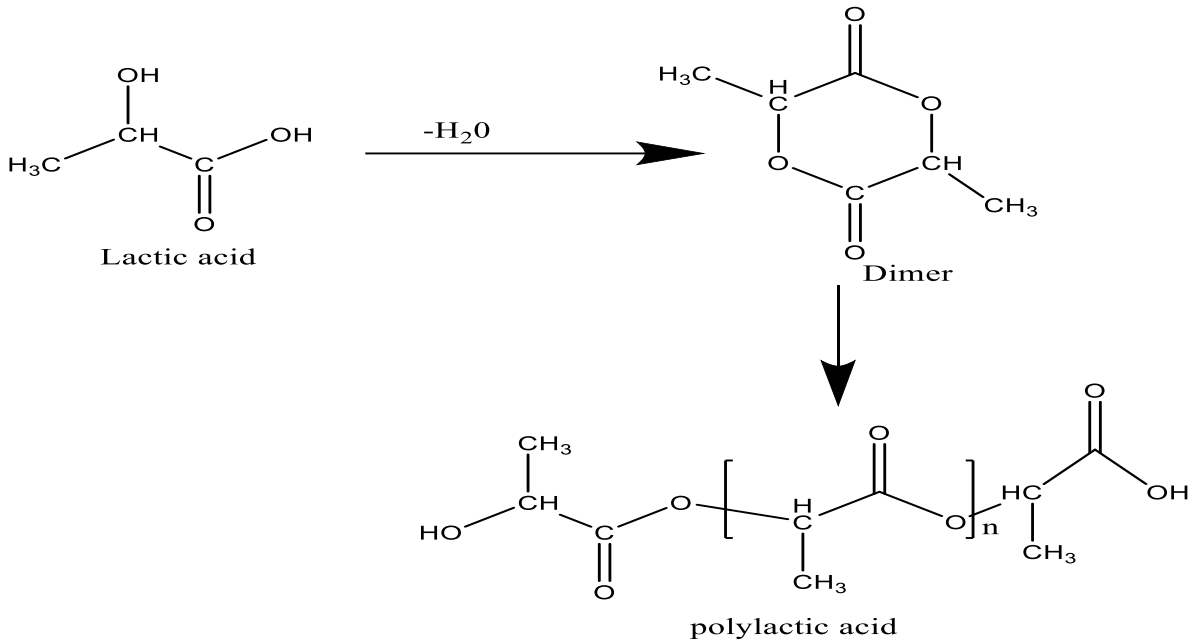

Scheme 1.2 Preparation of PLA from LA

Because of the presence of a chiral carbon in lactic acid, the monomer of PLA can have two unique arrangements (D-(dextro) or L-(levo)), and the relative properties and dissemination of these stereo isomers impacts difference properties of the PLA. Poly lactic acid containing L-lactic acid is termed as Poly L-Lactic Acid (PLLA) while PLA containing D-Lactic acid is referred as Poly D-Lactic Acid (PDLA), whereas PDLLA for isomers containing both L and D lactic acid.[24] Schematic description of polylactic acid is given in Figure 1.3

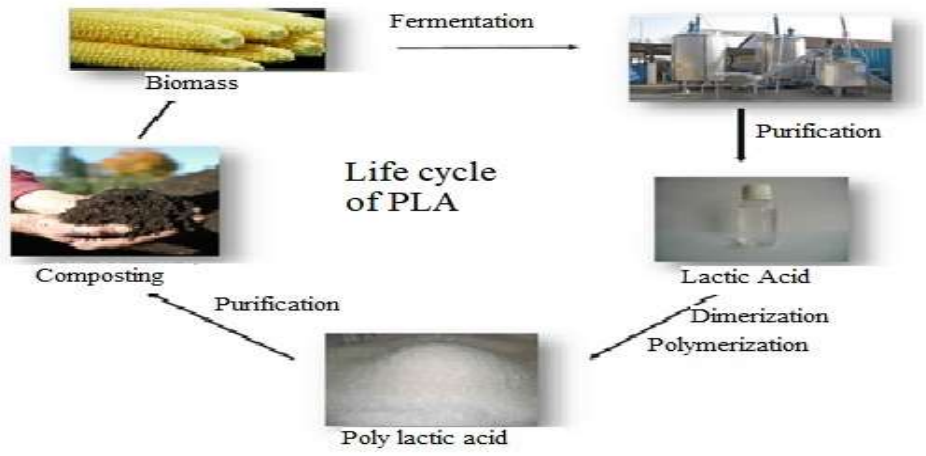

Figure 1.3 Schematic description for the preparation of PLA from biomass

It is realized that farming crude materials, for example, sugarcane or corn can be utilized as essential materials in PLA synthesis. It was said that PLA can be handled like all other thermoplastic polymers with expulsion, infusion forming, blow shaping, thermoforming, or fiber turning forms into different items.[25] PLA is a hardened and fragile polymer inferable from its high glass transition of 55^0C and melting point around 170^0C. But the melting point of PLA is dependent on nature of monomer either L-lactic acid or D-lactic acid. Due to good mechanical and stiffness properties PLA is used to make nano composite with nanomaterials. Table 1.1 for mechanical properties of PLA is

Table 1.1 Mechanical properties of Poly Lactic Acid (PLA)

Properties	**Values**
Young's modulus (MPa)	**3,600**
Flexural strength (N/mm2)	**98**
Tensile strength (MPa)	**70**
Elongation at break (%)	**2.4**
Density (g/cm3)	**1.25**
Moisture absorption (%)	**0.3**

In PLA, repeating unit is lactic acid in which C atom is chiral, having four different environments.

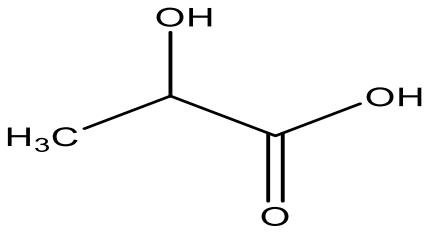

Lactic acid

1.4 CNT Functionalization

Functionalization have different kinds depending upon nature of interaction of CNT with polymer. It may be covalent or non-covalent, covalent functionalization is arises due to

covalent bond formation b/w CNT and polymer at the edges or center of CNT, while in non-covalent functionalization polymer is adsorbed on the surface of CNT due to π stacking and Van der Waals interaction. Both of them are exohedral in their nature influencing surface of tube but in endohedral small atoms are enter inside nanotubes.[26] [27] [28] Fig 1.3

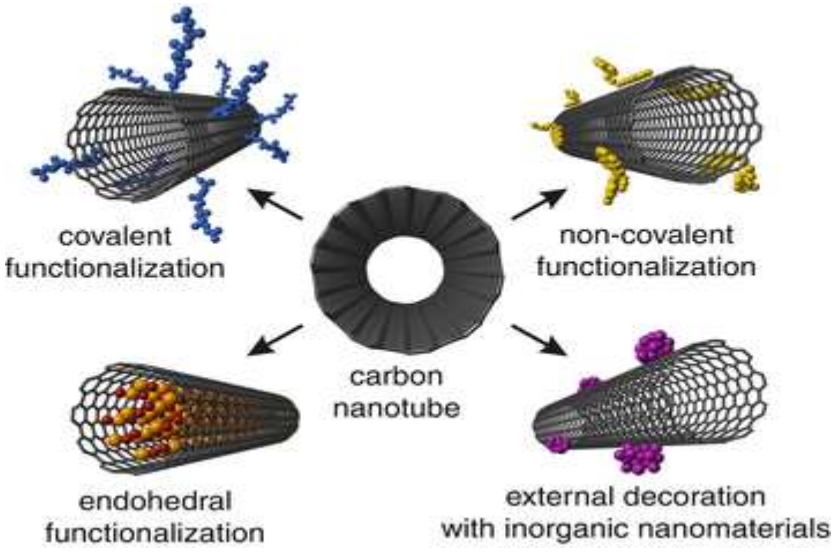

Figure 1.4 Covenant and non- covalent functionalization of CNT

1.5 Computational chemistry

Computational science is a cutting edge field of science that used Personal Computer (PC) In Computational science different calculations and conditions are utilized for solving unraveling substance issues.[29] Computational science is a solid creation that assists with foreseeing the different properties of the atoms that can't be conceivable practically. In addition, it assists with helping the trial science to make sense of the whole novel undertaking of chemistry. It expand the concept of theoretical chemistry and emerge them in computer technology like density functional theory, molecular dynamic simulation, molecular mechanics.ab-initio method and semi empirical method.[30] [31]

1.5.1 Density functional theory

Among electronic structure method, DFT is considered to be the most reliable approach to study the CNT/PLA composite. DFT approach is frequently utilized in material sciences, chemistry and physics to explore the electronic structure techniques for many body

framework.[32] [33] [34] It has ability to calculate electronic and thermodynamic parameter of molecular systems based on Kohn and sham's theory explaining the density of electron and wave functions.[35]

$$E = E_{(V)} + E_{(T)} + E_{(J)} + E_{(XC)} \qquad \text{Equation 1-1}$$

Where:

$E_{(V)}$ total potential energy of many body electronic system

$E_{(T)}$ kinetic energy

$E_{(J)}$ Repulsion energy b/w two electrons

$E_{(XC)}$ correlation exchange energy of electron

On the basis of approximation, DFT is classified into two methods

- LDA (Local Density Approximation)
- GGA (Generalized Gradient Approximation)

Local Density Approximation

In DFT, LDA is class of approximation to exchange correlation energy and depend upon each point in space and the value of electronic density, for example differentiation of density of kohn-sham orbitals[36],exchange correlation energy is written as

$$E^{LDA}(\mathrm{p}) = \int p(r)\, \varepsilon_{xc}\, (p(r))\, dr \qquad \textit{Equation 1-2}$$

Where:

p is the electronic density

ε_{xc} is exchange correlation energy per particle

Exchange correlation energy is further split into correlation terms and exchange linearly

$$E_{xc} = E_x + E_c \qquad \text{Equation 1-3}$$

Generalized Gradient Approximation

GGA is an expansion estimation of LDA for non-uniform electron thickness computations. GGA connection vitality strategy is most appropriate to contemplate the association between at least two molecules[30]

CHAPTER 2

LITERATURE REVIEW

2 Literature review

Due increasing demand of nano materials in technology many researcher worked on nano materials to explore and enhanced its properties by making composite. Following literature showing the importance of nano material and its composite

2.1 Electronic transport and conductivity

Donghui zhong *et al* synthesized Poly L-Lactic acid (PLLA) and Multiwall carbon Nano tube (MWCNT) composite using solution mixing and precipitation method and characterized them by Raman spectroscopic technique. They find electronic transport, Bio-compatibility and thermal properties of PLLA/MWCNT composite. Figure 2.1 showing relation b/w conductivity and loading of MWCNTs

In their work they observed that PLLA and MWCNT interaction occur due to hydrophobic interaction of C-CH_3 bond which indicate the formation of composite. Their work suggest that when loading of MWCNT is increased their conductivity is enhanced i.e., when they loaded 14% wt MWCNT to composite their conductivity is increased by 0.2 Scm^{-1}. From above graph it is clear that by increasing loading of MWCNT their conductivity is increased. Also their work suggest that growth of fibroblast cell was stopped due to presence of MWCNT.[26]

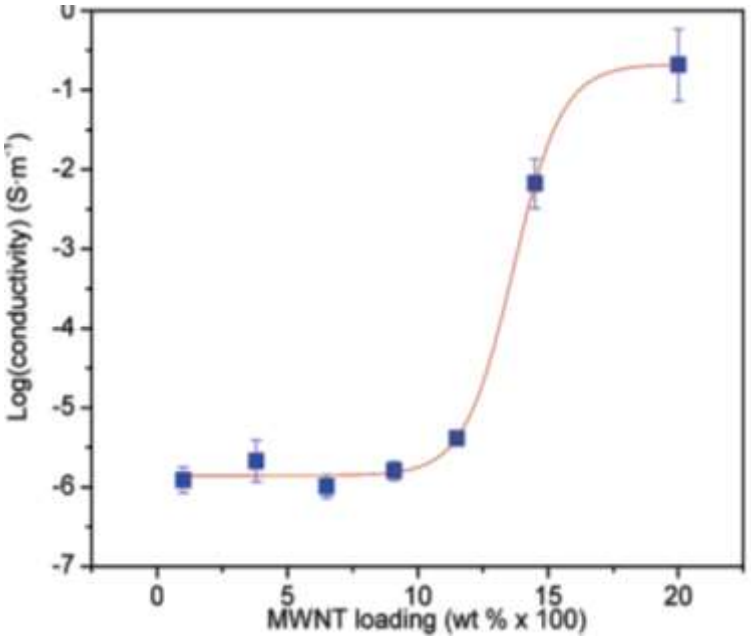

Figure 2.1 Relation b/w conductivity and loading of MWCNT

2.2 Effect of solvation on composite binding

Ahmed *et al* investigated the interaction of organic oligomers with Single Wall Carbon Nano Tube (SWNT) in the presence of polar and non-polar solvents for different dimensions of CNTs. Their main goal was to achieve the comparison of the result of interaction of organic oligomers with CNTs in two solvents, polar and non-polar and for different diameter of CNTs. Organic oligomers used for interaction are 9,9- dioctyl-9H-fluorene(FLU), 4,5-bis(decylthio)-dithiafulvene(DDTF) and 1,4-bis(decyloxy) Benzene(BDOB) shown in Fig-1.They used Gaussian16 builder for optimization of CNTs and their composite using three D-DFT dispersion corrected method WB97XD, B97D and B3LYP-D3 and basis set 6-31 G(d), 6-31++G(d,p). Fig 2.2 showing the structure of organic compounds

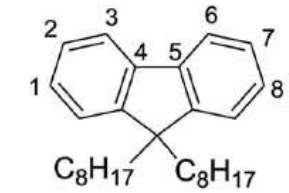

9,9-dioctyl-9*H*-fluorene
(FLU)

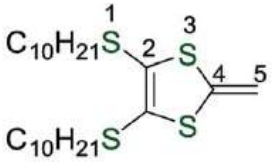

4,5-bis(decylthio)-dithiafulvene
(DDTF)

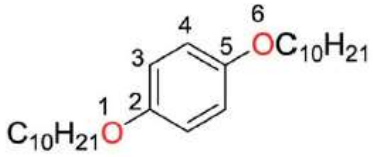

1,4-bis(decyloxy)benzene
(BDOB)

Figure 2.2 Sturucture of 9,9- dioctyl-9H-fluorene(FLU), 4,5-bis(decylthio)-dithiafulvene(DDTF) and 1,4-bis(decyloxy) Benzene(BDOB)

In their work they noticed that Organic oligomers are strongly interact on the suface of CNTs in the presence of polar solvents(Chlorofrom) while weekly interact in non-polar solvents, and in case of CNTs with small diameters binding energies are more than CNTs having largrer diameter.[37] Fig 2.3 showing interaction of oligomers on the surface of CNTs

2.3 LA-CNT Interaction and Density of states (DOS)

Alireza *et al* used DFT method to investigate the adsorption of lactic Lcid(LA) on the surface of CNTs, he took armchair(n=m) for their study.They appplied hybrid DFT method with

inclusion of dispersion correction and results was compared with non-corrected DFT method.They used Dmol3 on material studio and Gernalized gradient approximation method with double zeta basis set.The minimum adsorption energy of -13.39 kcal/mol was observed for LA on the surface of CNTs throgh hydroxl group of LA.Fig-3

They also percieve the density of states(DOS) and projected density of states (PDOS) which demonstrate that electronic state was granted by CNTs rahther tha LA.Fig 2.4 showing interaction of lactic acid on the surface of CNTs.

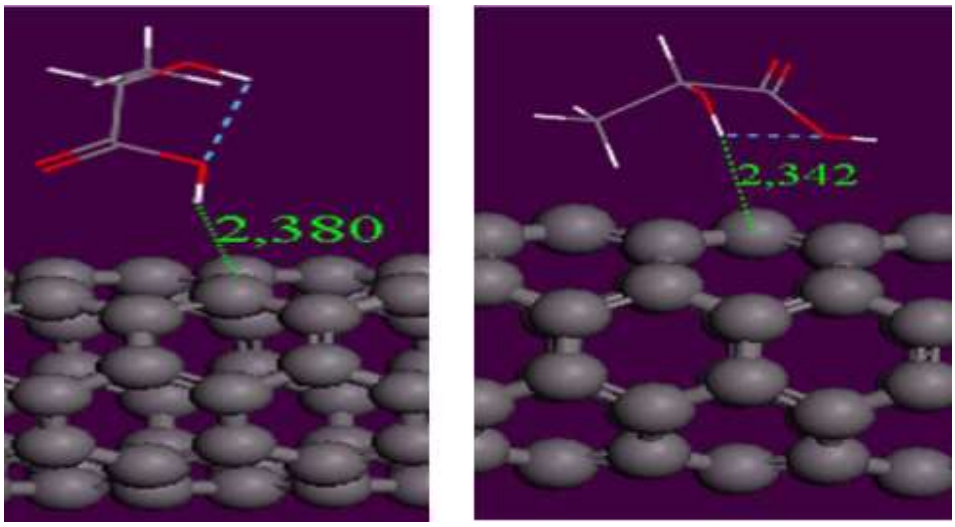

Figure 2.3 Interaction of Lactic Acid (LA) on CNT

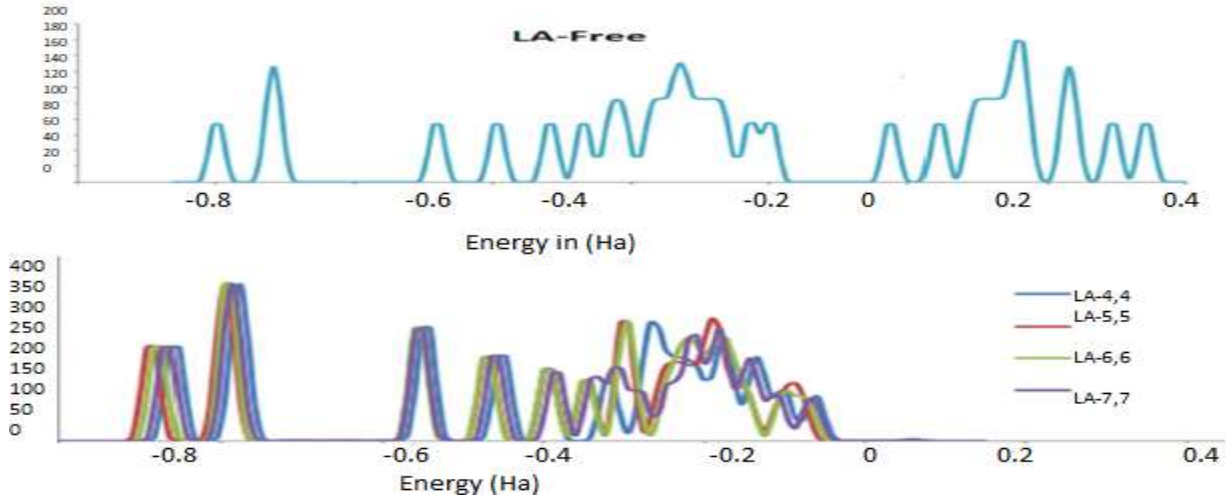

Figure 2.4 The total density of states of free lactic lacid and adsorbed on SWCNTs

2.4 Thermal conductivity

Mohammad Alaghemandi *et al* explored the thermal conductivity of Single Wall Carbon Nano Tube (SWCNT) and poly Amide (PA) composite by employing reverese non-equilbrium Moleculer Dynamic (RNEMD) simulation method and adjust atomistic rsolution.In their work they took 10nm length of SWCNT and four repeating unit of 6,6-polyamide of polymer in unit cell. The temprature of the system was taken 350K and coupling time of 1ps.After performing MD simulation they observed that thermal conductivity of composite was enhanced parrallel to CNT but decrease in the direction of perpendicular to CNT, because when PA was oriented parrallel to CNT, interfacial thermal resistance b/w CNT and polymer was more inflated than in perpendicular direction. [38] Figure 2.6

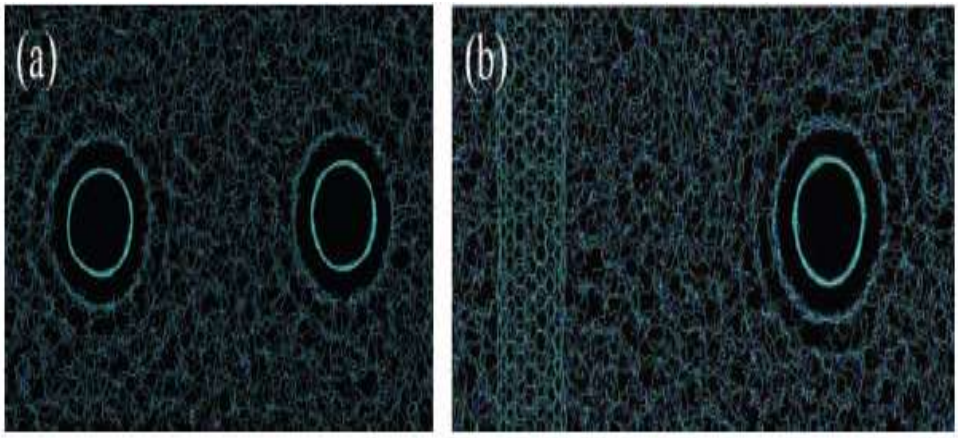

Figure 2.5 An xz projection of simulation cell either with two parallel (a) or two perpendicular (b) CNTs in the nanocomposite

2.5 Mechanical properties of CNT-PE composite

Frankland *et al* found out the stress-strain cuve of Carbon nano tube embeded with polyethylene CNT/PE using Molecular dynamic(MD) simulation. For their work they took an armchair of 10,10 and polyethylene polymer having eight chain of $–CH_2-$ with 1095 repeating units.Thy compared the stress-strain curve of composite with long continous CNT and short discontinious CNT.In their work they noted that composite with long chain continous CNT allow more loading Fig 2.7 than short CNT because long continous CNT have more aspect ratio than short CNT. [39] Fig 2.8

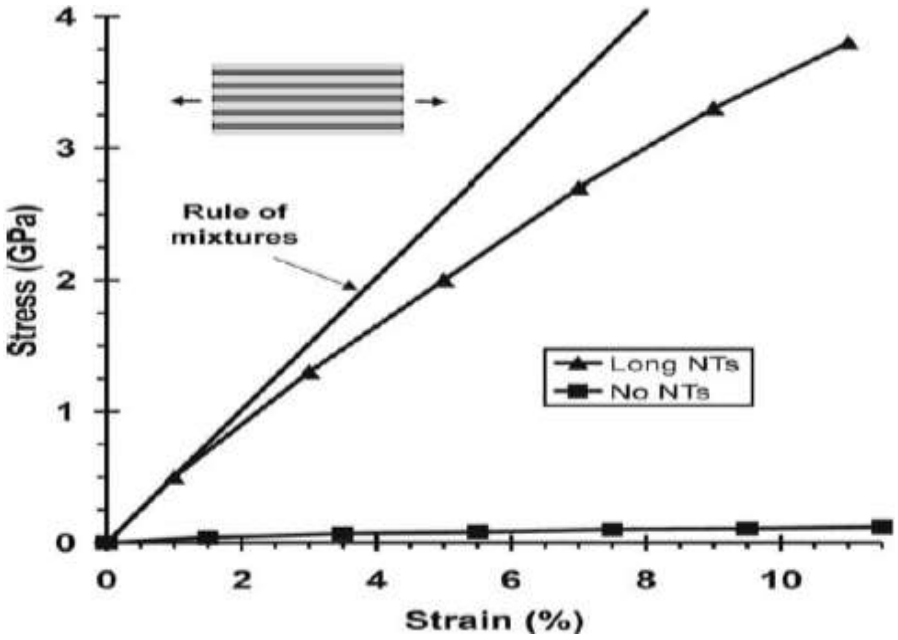

Figure 2.6 Graph between Stress and strain of CNT/PE composite

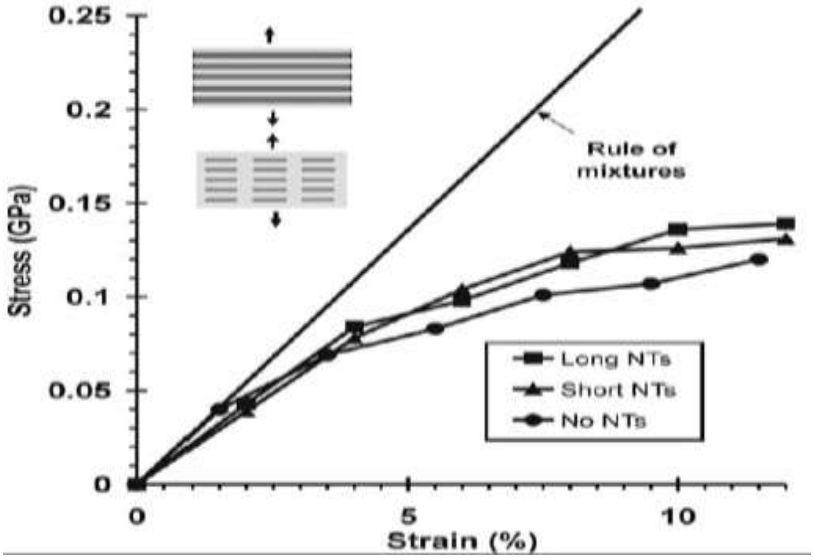

Figure 2.7 Graph between stress and strain of long and short NTs

2.6 Problem statement

Metallic conductor being used in mechanical industry limit their scope on account of heavy weight, safety and corrosion phenomena. Replacing CNT composite for energy transfer along with high mechanical strength leads to corrosion reduction enhancing desirable perspective.

2.7 Objectives

Main objectives of current research are

- Design of cross linked PLA to study the effect of PLA on DOS, energy gap, band structure and energetic parameter of CNTs.
- To find out the strength of CNT/PLA composite based on adsorption energy and adsorption constant.
- To study effect of PLA on electrical, mechanical and thermodynamic properties of CNT's.

2.8 Preface & significance of research

Carbon nano tube is very expensive and if we used it in experiment and our result are not favorable then it is loss of chemicals, time and money. My work have much importance because computationally i find out suitable path way for the adsorption of PLA on surface of CNTs and investigated the properties of CNT/PLA composite on the basis of adsorption energy and adsorption constant. Computational data tell us how to adsorb PLA on the surface of CNTs.

.

Chapter 3

Methodology

3 Methodology

To study the adsorption behavior of PLA on CNTs, the first step is to design different dimensions of CNTs. Avogadro's builder is efficient because multiple CNTs with different dimensions with variable orientations can be designed. Avogadro builder is considered as powerful editor to produce nano materials including polymers, organic structure and CNTs with high visualization.

Presently ten CNTs of arm chair [(2,2), (3,3), (4,4), (5,5)], Chiral [(2,3), (3,4),(4,5)], Zigzag [(3,0), (4,0), (5,0)] are build using this builder for the adsorption of PLA on the surface of CNTs.[40]

ADF is considered as a powerful tool to investigate the adsorption behavior, electronic parameter, frequency calculation in material sciences, chemistry and quantum physics.

Constrained Optimization of PLA, CNT and CNT/PLA

Presently three different kind of CNTs arm chair : (2,2), (3,3), (4,4), (5,5) , chiral :(2,3), (3,4), (4,5) and zigzag : (3,0), (4,0), (5,0) are built from Avogadro builder and then optimized before the using DFT theory employing GGA approach and PW91basis set. Double zeta basis and medium frozen core along with good numerical quality is chosen for parametric calculations. On the basis of constrained optimization calculations electronic and energetic parameters provided an estimation of electron donating and accepting regions of CNTs for providing suitability of adsorbate attack.

PLA is built by using cross-linking polymerization process, taking three monomers with cross linking of three repeating unit of LA and set to lowest possible energy conformation. Corss-linked PLA structure is adsorbed on edges and center position of the surface of CNTs. Results are compared with parent CNTs to determine adsorption energy. Optimized structure of one dimension of CNT/PLA composite is shown Figure 3.1

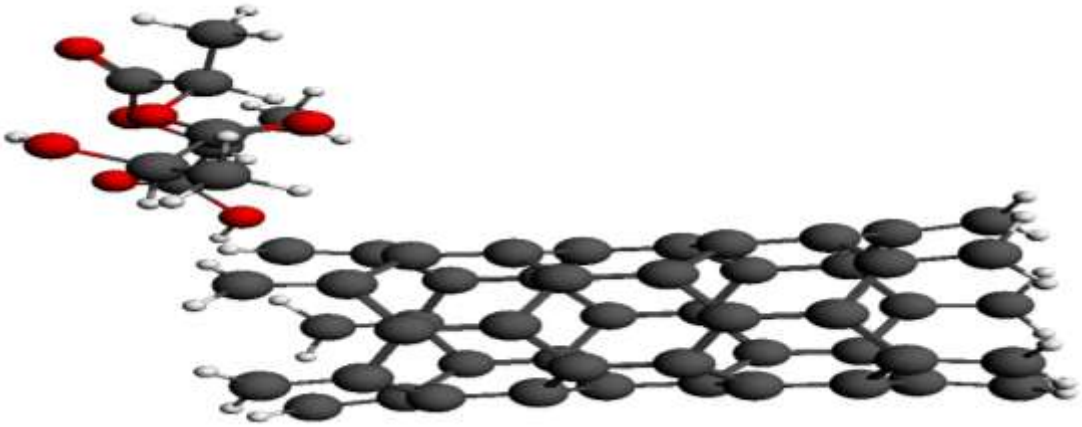

Figure 3.1 optimized structure of CNT/PLA composite

Frequency Calculations

Frequency calculation is performed for CNT/PLA composite to calculate the electrical conductivity of CNT/PLA composite. In frequency calculation enthalpy (ΔH) and heat capacity at constant volume (C_V) is determined to find the adsorption constant (Kd) and Gibbs free energy (ΔG). Adsorption constant (Kd) have been calculated from adsorption energy (ΔE), the formula for Kd is given in Equation 3-1

$$Kd = e^{-\Delta E/RT} \qquad \text{Equation 3.1}$$

Where

K_d is adsorption constant

ΔE Is adsorption energy

R is general gas constant, its value is 0.008315 $kJmol^{-1}$

T is absolute temperature, its value is 273.16 K

Calculation of Energy gap and electrical conductivity

Energy gap b/w HOMO and LUMO have been calculated by taking difference between them. Electrical conductivity is calculated using ΔE in equation 3.2

$$\Delta E = E_{HOMO} - E_{LUMO} \quad (3.2)$$

Electrical conductivity is conduction of electron from valence band to conduction band, lesser the energy gap b/w these band more will be electrical conductivity. Electrical conductivity is dependent on exponential function of ΔE, Equation 3.3

$$\sigma = e^{\Delta E/2kbT} \quad (3.3)$$

Where

σ Is electrical conductivity in Sm^{-1}.

k_b is Boltzmann constant

T is absolute temperature

The flow chart for Adsorption of PLA on the surface of CNTs is described below

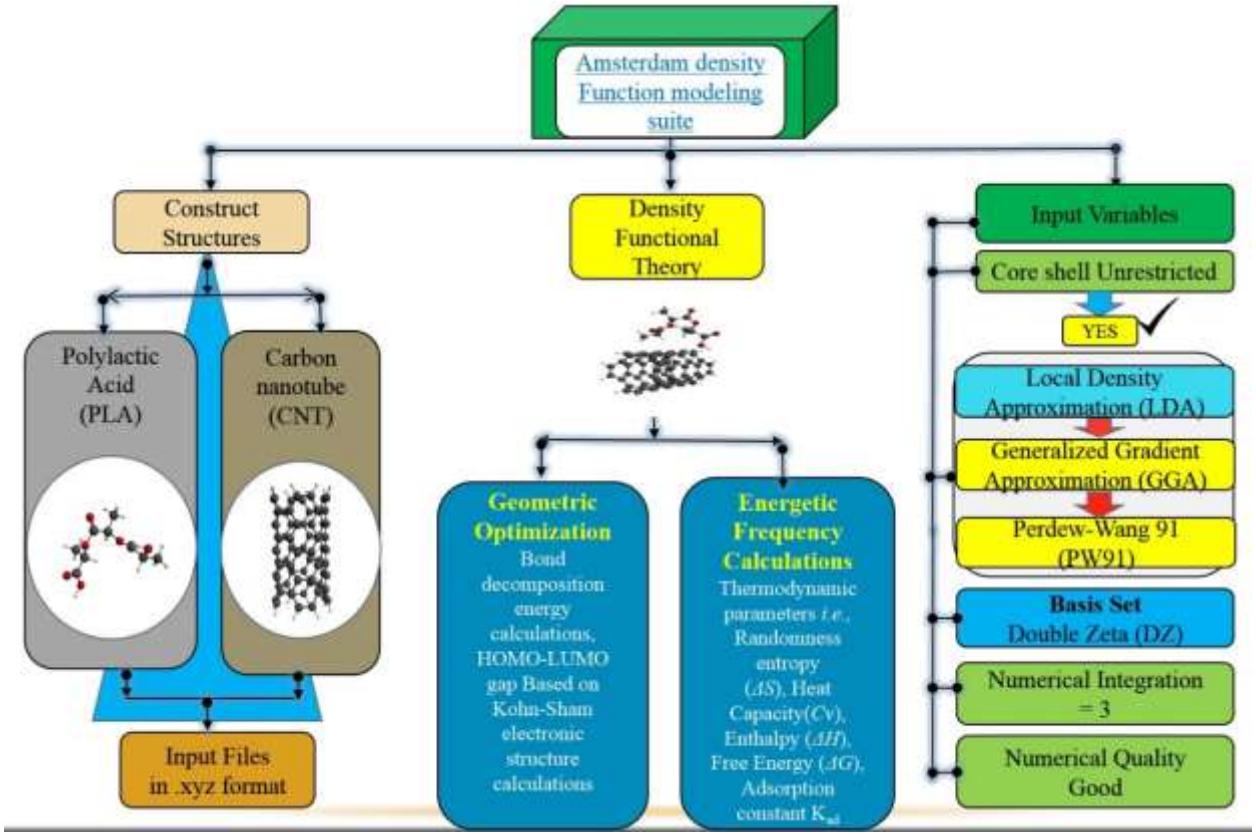

Figure 3.2 Flow chart for computational modeling of CNT/PLA composite

Chapter 4

Result & Discussion

4 Result and discussion

Presently three different CNTs, Armchair having dimensions of (2,2), (3,3), (4,4),(5,5),Chiral having dimensions of (2,3), (3,4),(4,5) and zigzag of dimensions (2,0), (3,0), (4,0), (5,0) are selected for the adsorption of poly lactic acid on the surface of CNTs using DFT study. Electronic , thermodynamic and mechanical parameters were calculated to determine the favorable interaction of poly lactic acid on the surface of CNTSs. Reversible reaction are associated with physio sorption having negative value of E_{ads} while positive value of E_{ads} are associated with chemisorption.[41 42]

$$E_{ads} = E_{CNT/PLA} - (E_{CNT} + E_{PLA})$$

Where $E_{CNT/PLA}$ is energy of composite and E_{CNT} and E_{PLA} energies of CNTs and poly lactic acid respectively. To find morphological properties of CNTs/PLA composite, we evaluated the geometric parameter before and after adsorption, adsorption energy (E_g), Adsorption constant ($K_{d)}$, Enthalpy (ΔH), Entropy (ΔS), Gibbs free energy (ΔG) young modulus (ΔY) and energy gap (ΔE) b/w HOMO and LUMO.

4.1 Kinetic and electronic effect of adsorption

Presently ten CNTs are selected with different dimension are selected for the adsorption of PLA on its surface. To investigate the kinetic and electronic parameter of CNT/PLA composite adsorption constant (K_d) ΔE for HOMO and LUMO is calculated.

PLA is adsorbed on different orientation of armchair CNTs and compare the energy gap for the adsorption at center and edges of surface of CNTs. Greater energy gap showing strong binding. Computational data revealed that stronger binding is observed in arm chair is for 4, 4 CNTs in both cases, adsorption at center as well as at edges of surface of CNTs .Because in both cases PLA shared its electron towards CNTs and made strong bonding. Adsorption constant for 4, 4 CNT/PLA composite at center and edges are 2.7458×10^{20} and 5.4557×10^{10}. Among chiral and zigzag the strong binding is observed for 2, 3 and 4, 0 respectively. They have k_d value of 6.4321×10^{8} and 2.6897×10^{21} respectively Figure 4.1 (A-D) showing the adsorption of PLA on the edges of CNTs and Figure 4.2 (A-D) showing the adsorption of PLA on the center of CNTs.

Table 4.1 Energetic parameter, adsorption energy and adsorption constant values of CNT/PLA composite

Arm chair

Adsorption of PLA on center of CNTs

CNTs	E_{CNT} kj/mol	E_{PLA} kj/mol	$E_{CNT+PLA}$ KJ/mol	ΔE_g kj/mol	K_d (M^{-1})
2,2	-29970.00	-16328.18	-46388.16	-89.98	1.6403×10^{17}
3,3	-47431.25	-16328.18	-63806.80	-47.37	1.1556×10^{9}
4,4	-64454.57	-16328.18	-80889.58	-106.83	2.7458×10^{20}
5,5	-81309.82	-16328.18	-97714.79	-76.79	4.9139×10^{14}

Arm chair

Adsorption of PLA on edges of CNTs

CNTs	E_{CNT} KJ/mol	E_{PLA} KJ/mol	$E_{CNT+PLA}$ KJ/mol	ΔE KJ/mol	K_d (M^{-1})
2,2	-29970.00	-16328.18	-46298.18	-32.21	1.4534×10^{6}
3,3	-47431.25	-16328.18	-63759.43	-19.08	4.470×10^{3}
4,4	-64454.57	-16328.18	-80782.75	-56.12	5.4557×10^{10}
5,5	-81309.82	-16328.18	-97686.55	-48.55	1.9434×10^{9}

Table 4.2 Energetic parameter, adsorption energy and adsorption constant values of CNT/PLA composite

Chiral

Adsorption of PLA on center of chiral CNTs

CNTs	E_{CNT}	E_{PLA}	$E_{CNT+PLA}$	ΔE KJ/mol	K_d (M^{-1})
2,3	-36593.41	-16328.18	-52967.63	-46.04	6.4321×10^{8}
3,4	-52044.43	-16328.18	-68397.44	-24.83	5.6294×10^{4}
4,5	-67235.40	-16328.18	-83599.85	-36.27	8.6928×10^{6}

Zigzag

Adsorption of PLA on center of zigzag CNTs

CNTs	E_{CNT}	E_{PLA}	$E_{CNT+PLA}$	ΔE KJ/mol	K_d (M^{-1})
4,0	-32081.41	-16328.18	-48521.60	-112.01	2.6897×10^{21}

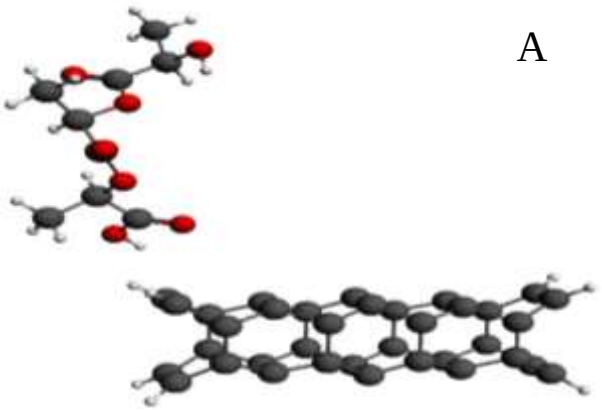

A

Interaction of PLA on the edge of 2, 2 CNT

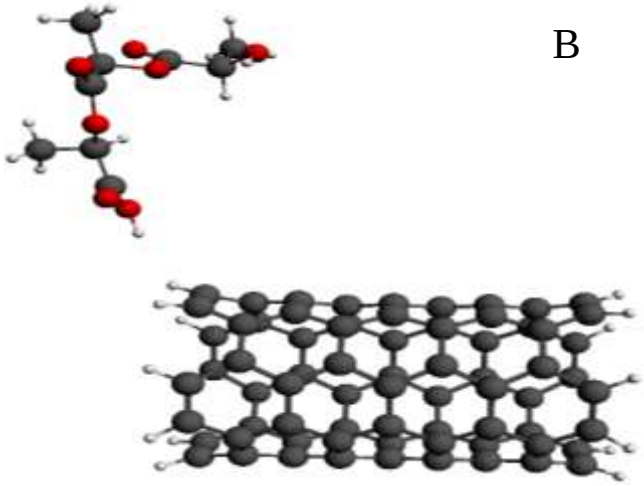

B

Interaction of PLA on the edge of 3, 3 CNT

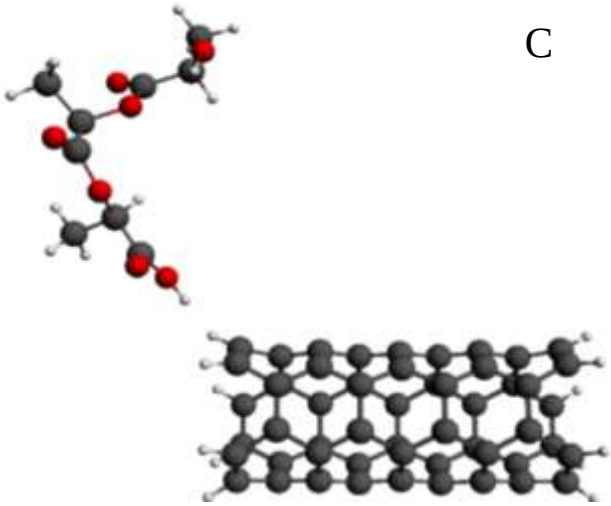

C

Interaction of PLA on the edge of 4, 4 CNT

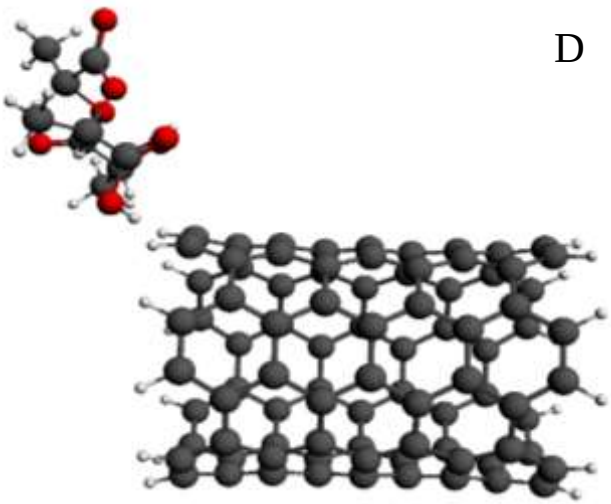

D

Interaction of PLA on the edge of 5, 5 CNT

Figure 4.1 (A) Interaction of PLA on the edge of 2, 2 CNT (B) Interaction of PLA on the edge of 3, 3 CNT (C) Interaction of PLA on the edge of 4, 4 CNT (D) Interaction of PLA on the edge of 5, 5 CNT

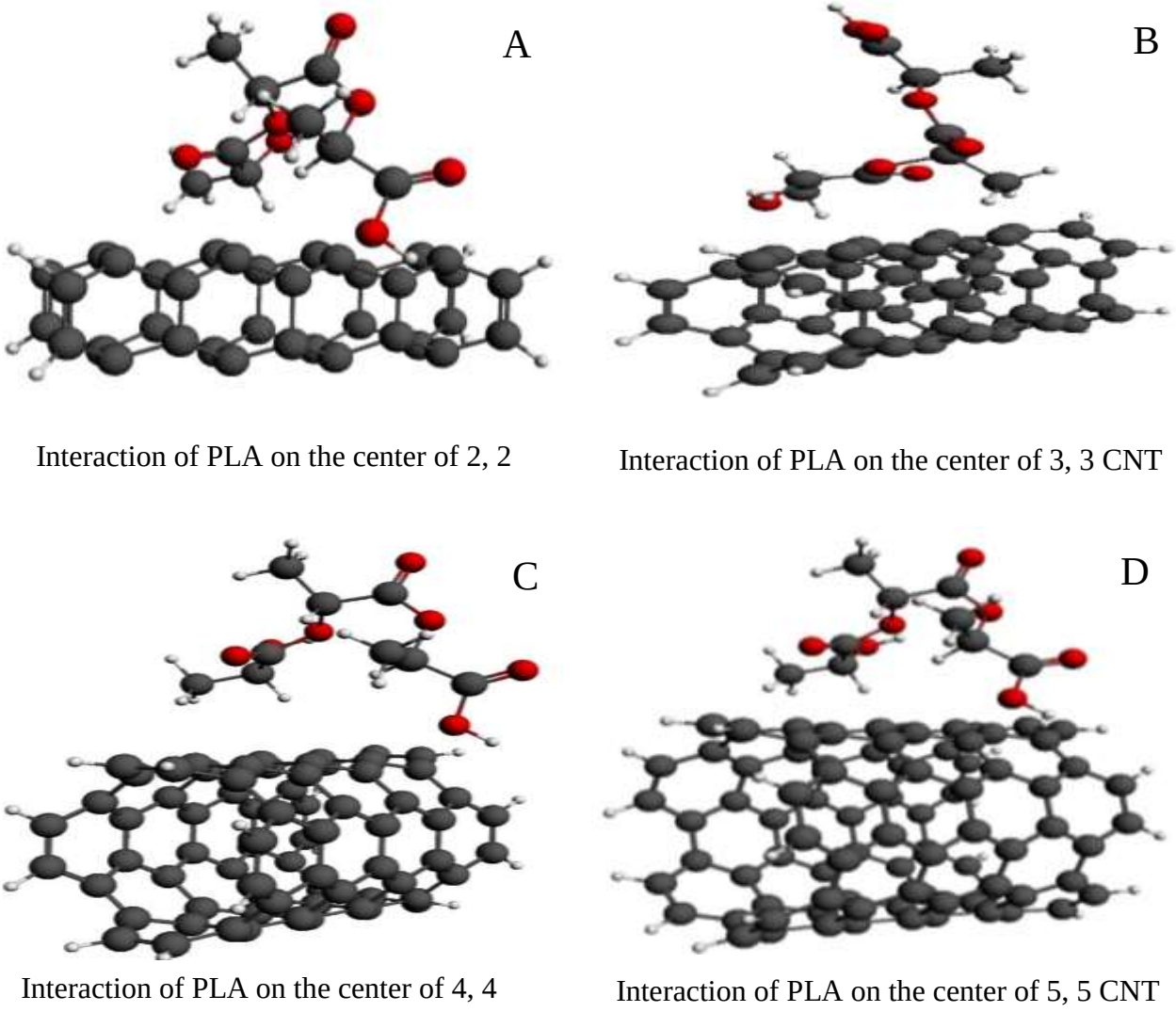

Interaction of PLA on the center of 2, 2

Interaction of PLA on the center of 3, 3 CNT

Interaction of PLA on the center of 4, 4

Interaction of PLA on the center of 5, 5 CNT

Figure 4.2 *(A)* Interaction of PLA on the center of 2, 2 CNT (B) Interaction of PLA on the center of 3, 3 CNT (C) Interaction of PLA on the center of 4, 4 CNT (D) Interaction of PLA on the center of 5, 5 CNT

4.1.1 Stability of composite based on E_{HOMO} - E_{LUMO} gap

The energy gap b/w HOMO and LUMO play important role in the stability of composite, smaller energy gap significance stronger interaction and high reactivity of CNTs with PLA. From computational data the lesser energy gap is observed for an arm chair of dimension 4, 4 CNT/PLA composite, 0.60 eV and 0.61 eV respectively for both, adsorption at center as well as on the edges of CNTs

Among chiral and zigzag CNTs less energy gap is observed for 2, 3 and 4, 0 CNT/PLA composite that is 1.04 and 0.26 eV. The highest energy gap is 1.81 eV observed for 3, 4

CNT/PLA. Computational data and HOMO, LUMO gap is shown in table 4.3 and Fig 4.2 to 4.4 respectively.

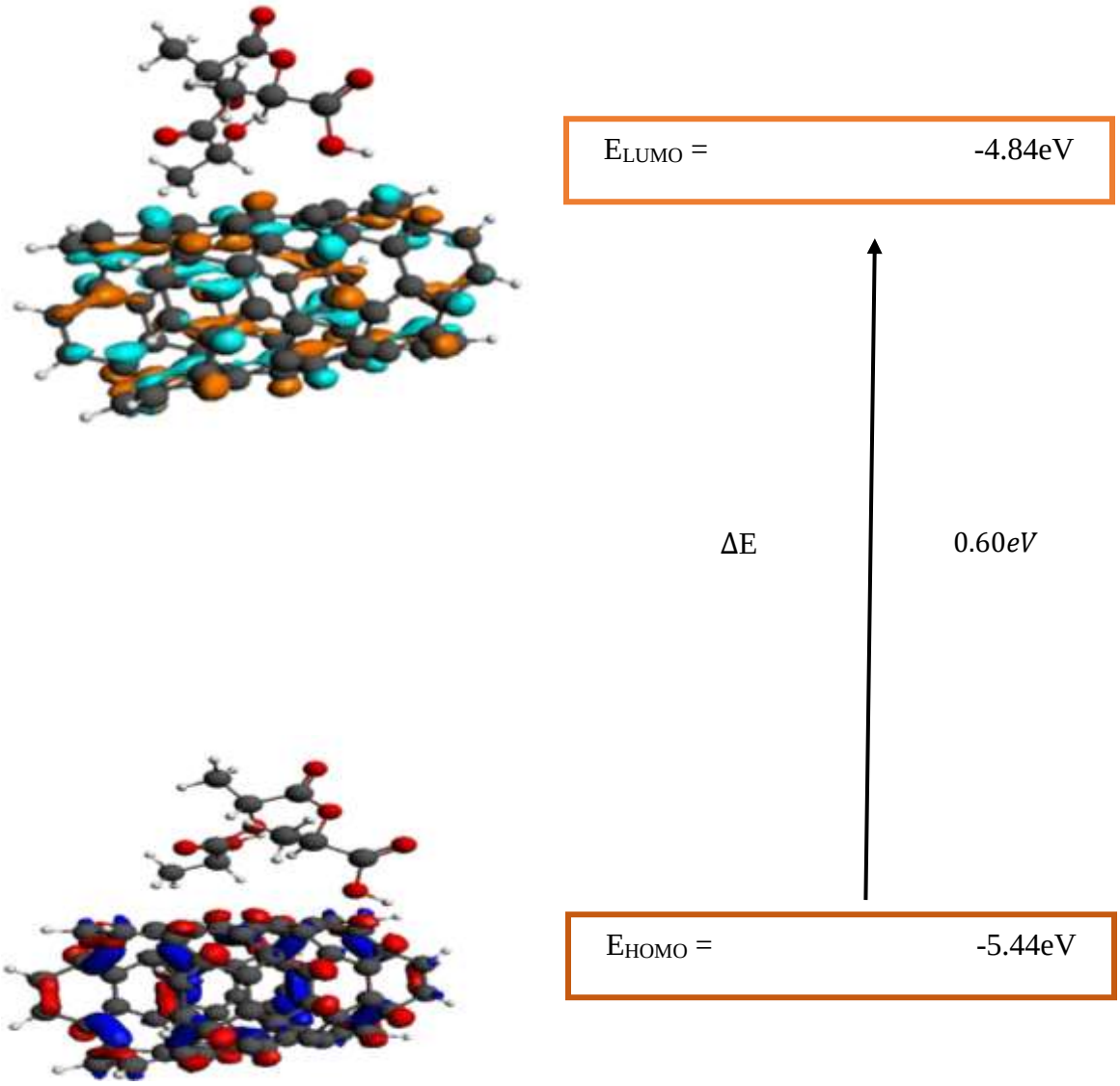

Figure 4.3 HOMO - LUMO gap of 4, 4 CNT composite (adsorption at center /PLA)

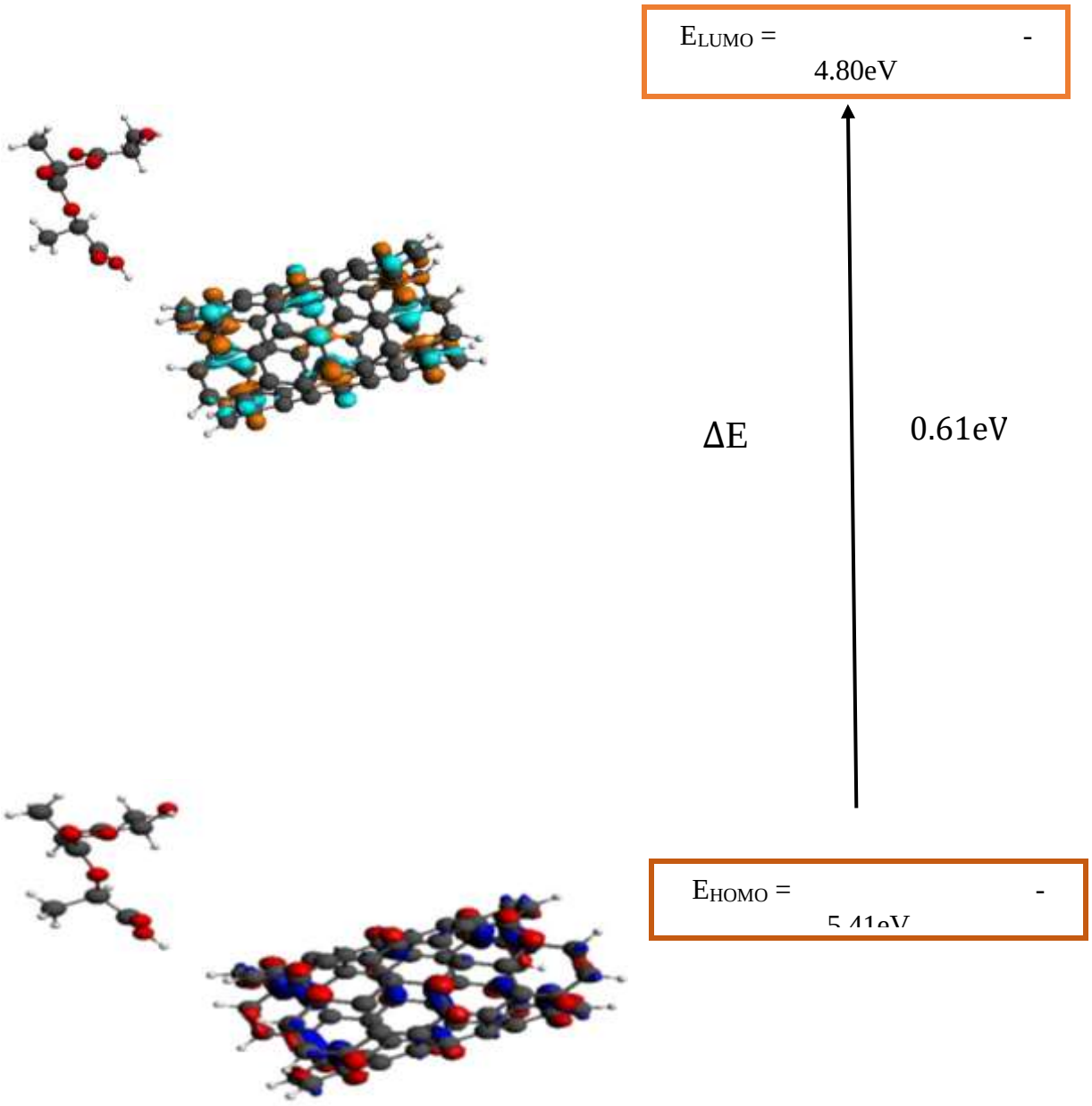

Figure 4.4 HOMO - LUMO gap of 4, 4 CNT/PLA (adsorption at edge) composite

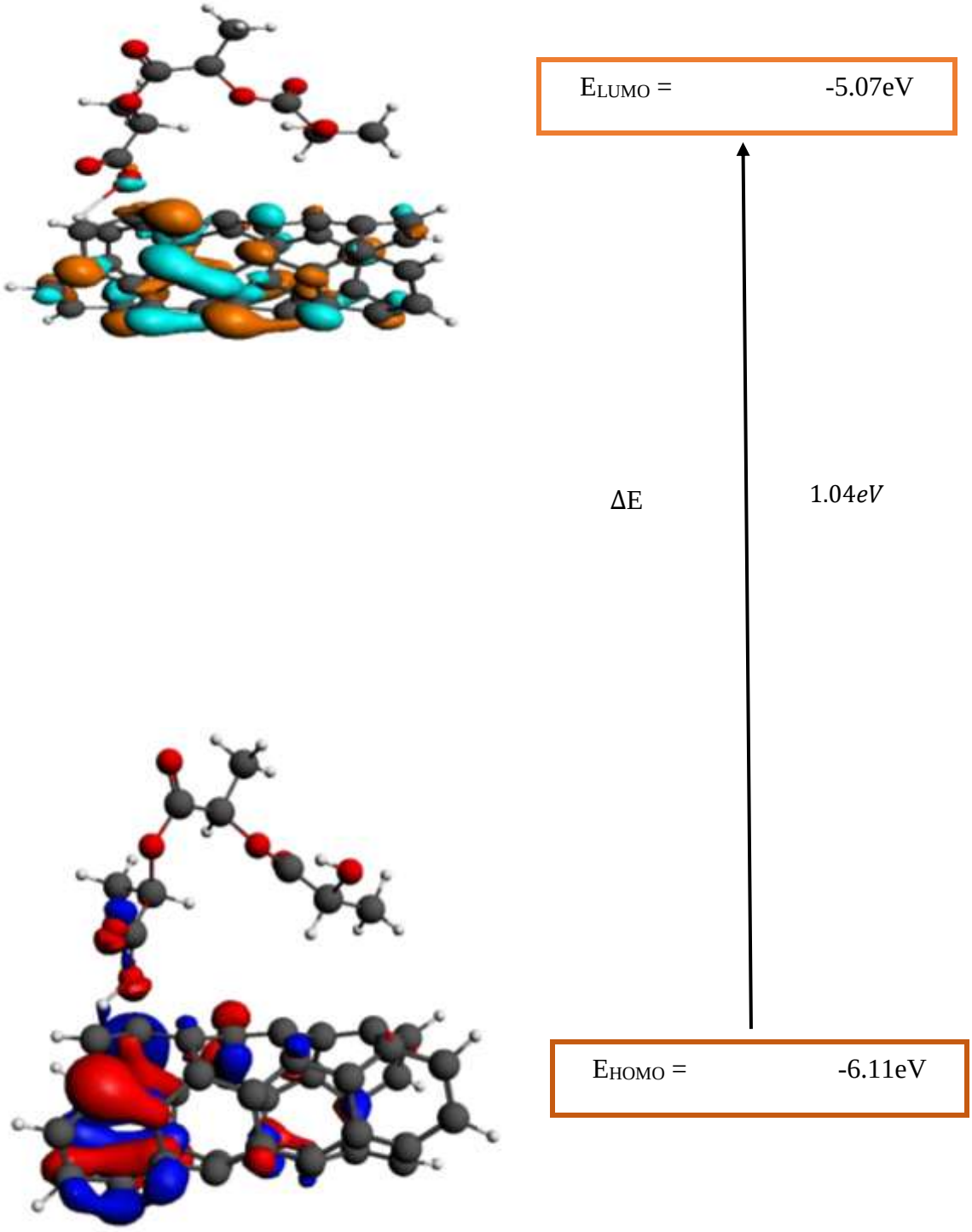

Figure 4.5 HOMO - LUMO gap of 2, 3 CNT/PLA (adsorption at center) composite

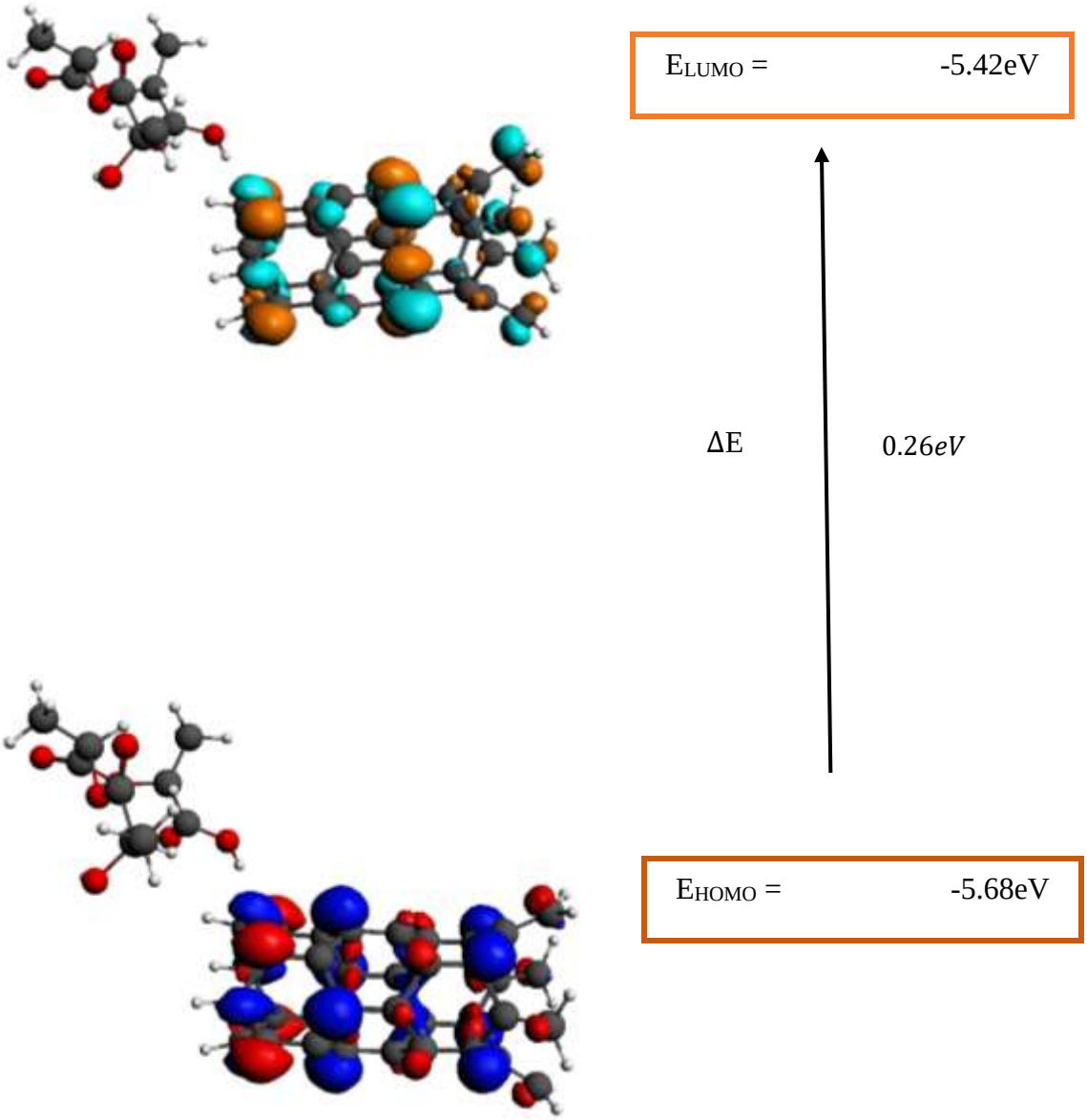

Figure 4.6 HOMO - LUMO gap of 2, 3 CNT/PLA (adsorption at center) composite

Table 4.3 Energy gap after interaction of PLA on CNTs

S.NO	E_{HOME} eV	E_{LUMO} eV	$\Delta E = E_{HOME} - E_{LUMO}$ eV
4,4 CNT/PLA (adsorption at center)	-5.44	-4.84	0.60
4,4 CNT/PLA (adsorption at edges)	-5.41	-4.80	0.61
2,3 CNT/PLA (adsorption at center)	-6.11	-5.07	1.04
4,0 CNT/PLA (adsorption at center)	-5.68	-5.42	0.26

4.2 Kinetic and thermodynamic effect of adsorption

Thermodynamic parameter including enthalpy and entropy are calculated to check the spontaneity and more stable configuration of PLA/CNT composite, while Gibbs free energy explain the interaction b/w adsorbate and adsorbent. From calculated data greater enthalpy 347.9229 KJ mol^{-1} is observed for 5, 5/PLA composite and entropy value of 1.2141 KJ $mol^{-1}K^{-1}$ for same composite.

So 5, 5/PLA composite having more stable configuration because hydroxyl group attached to PLA is share its more electron density towards 5,5 CNT.

According to Boltzmann law of entropy

$$S = k \ln W$$

Where S is entropy and W shows the number of microstates and k is Boltzmann constant. From this law larger entropy have more number of microstates which make stable configuration of composite.

Poly lactic is an organic compound containing –COOH and –OH at terminal carbon compound, it interact with CNTs and shared its electron towards CNTs and make strong binding. Thermodynamic data prove strong binding is observed for 2, 2 CNT/PLA composite among Chiral CNTs because it have more negative Gibbs free energy and greater K_d constant.

Table 4.4 Thermodynamic data for the adsorption of PLA on the center & edges of surface of an arm chair CNT's calculated by GGA-PW91

Arm chair

Adsorption of PLA on center of armchair CNTs

CNTs /PLA	Enthalpy Kj/mole	Entropy KJ/mole K^{-1}	*Gibbs Free Energy* KJ/mol
2,2	180.1184	0.7715	-49.912
3,3	240.8834	0.9330	-37.2998
4,4	289.0363	1.046	-22.8390
5,5	343.5399	1.1849	-9.7498

Table 4.5 Thermodynamic data for the adsorption of PLA on the center of surface of the chiral CNT's calculated by GGA-PW91

Chiral

Adsorption of PLA on center of surface of Chiral CNTs

CNTs /PLA	Enthalpy Kj/mole	Entropy KJ/mole K^{-1}	*Gibbs Free Energy* KJ/mol
2,3	203.7029	0.8577	-52.0289

4.3 Electrical conductivity

The ability of any material to flow electrons is called conductivity. Conductivity of material depends upon energy gap b/w HOMO and LUMO (E_g) value.[43]

Relation between conductivity and Eg value is illustrated as

$$\sigma = e^{-\Delta E/2kT} \quad \text{Equation 4.1}$$

Where

$$\Delta E = E_{HOMO} - E_{LUMO} \quad \text{Equation 4.2}$$

Where σ Electrical conductivity, E_g is energy gap between HOME and LUMO in electron volts (eV), T is temperature in Kelvin and k is Boltzmann constant with value of constant = 1.380×10^{-23} $JK^{-1.}$

Before the adsorption of PLA on the surface of CNT, energy gap and electrical conductivity is find out. Computational data revealed that lesser energy gap is observed among arm chair for 5,5 CNT with greater electrical conductivity of $25.7 \times 10^{-7} Sm^{-1}$. Because of smaller energy gap the electron can easily be jump from valence band to conduction and conduct electricity. Table 4.6 showing the values of energy gap and electrical conductivity of CNTs.

For Chiral CNTs the lesser energy gap -1.04 eV is observed of 3, 4 and electrical conductivity of 25.3×10^{-17} Sm^{-1}, Because when PLA is adsorbed on the surface of chiral CNT the electrons are shared from PLA to CNT and energy gap of chiral is reduced.

Among Zigzag the lesser energy gap -0.26 eV and electrical conductivity of $39.7 \times 10^{-4}$is observed for 4, 0 CNT. Table 4.7 showing the values of energy gap and electrical conductivity of Chiral and zigzag CNTs

When PLA is adsorbed on the center of different dimensions of armchair CNTs e.g. (2, 2), (3, 3) (4, 4), (5, 5) the lesser energy gap -0.35 eV is observed for 5,5 CNT and more electrical conductivity among armchairs CNTs, that is 25.7×10^{-7}S/m. Among chiral and zigzag CNTs more less energy gas is observed for 2, 3 and 5, 0 CNTs/PLA composite having electrical conductivity 25.3×10^{-17} and 39.7×10^{-4} S/m respectively. Table 4.8 and 4.9 showing the electrical conductivity of CNTs/PLA composite.

Table 4.6 Electronic parameter of pure Arm chair and chiral CNTs.

Arm chair

CNTs	**E_{HOMO}/eV**	**E_{LUMO}/eV**	**$\Delta E = E_{HOMO} - E_{LUMO}$ /eV**
2,2	-5.9918	-4.87	-1.12
3,3	-5.6689	-4.4798	-1.20
4,4	-5.3391	-4.7406	-0.40
5,5	-5.2714	-4.9020	-0.36

Chiral

CNTs	**E_{HOMO} eV**	**E_{LUMO} eV**	**$\Delta E = E_{HOMO} - E_{LUMO}$/eV**
2,3	-6.3693	-4.8220	-1.54
3,4	-5.9350	-4.1263	-1.82
4,5	-5.7416	-4.2716	-1.47

Table 4.7 Electronic parameter and electrical conductivity of Zigzag CNT

CNTs	**E_{HOMO}/eV**	**E_{LUMO}/eV**	**$\Delta E = E_{HOMO} - E_{LUMO}$/eV**
3,0	-5.5505	-4.7627	-0.7878
4,0	-5.6355	-5.3208	-0.31
5,0	-4.7418	-3.4715	-1.27

Table 4.8 Electronic parameter and electrical conductivity (S/m) CNT/PLA composite (calculated: GGA; pw91, DZ basis set and good numerical quality)

Arm chair

Adsorption of PLA on center of armchair CNTs

CNTs /PLA	**E_{HOMO} /eV**	**E_{LUMO}/eV**	**$\Delta E = E_{HOMO} - E_{LUMO}$ /eV**	**$\Delta E = E_{HOMO} - E_{LUMO}$ J**	**$\sigma = e^{-\Delta E/2kT}$ S/m**
2,2	-5.89	-4.89	-0.97	1.55×10^{-19}	42.4×10^{-17}
3,3	-5.79	-4.26	-1.21	1.93×10^{-19}	41.4×10^{-21}
4,4	-5.41	-4.84	-0.60	1.07×10^{-19}	46.0×10^{-11}
5,5	-5.36	-4.94	-0.39	6.24×10^{-20}	25.7×10^{-7}

Armchair

Adsorption of PLA on edges of armchair CNTs

CNTs /PLA	**E_{HOMO}/eV**	**E_{LUMO}/eV**	**$\Delta E = E_{HOMO} - E_{LUMO}$/eV**	**$\Delta E = E_{HOMO} - E_{LUMO}$ J**	**$\sigma = e^{-\Delta E/2kT}$ S/m**
2,2	-5.89	-4.80	-1.09	1.74×10^{-19}	36.0×10^{-18}
3,3	-5.79	-4.59	-1.2	1.92×10^{-19}	49.6×10^{-20}
4,4	-5.41	-4.80	-0.61	9.77×10^{-20}	47.7×10^{-10}
5,5	-5.36	-4.92	-0.44	7.049×10^{-20}	35.9×10^{-7}

Table 4.9 Electronic parameter and electrical conductivity (S/m) CNT/PLA composite (calculated: GGA; pw91, DZ basis set and good numerical quality)

Chiral

Adsorption of PLA on center of surface of chiral CNTs

CNTs /PLA	**E_{HOMO}/ eV**	**E_{LUMO}/ eV**	**$\Delta E = E_{HOMO} - E_{LUMO}$/eV**	**$\Delta E = E_{HOMO} - E_{LUMO}$ J**	**$\sigma = e^{-\Delta E/2kT}$ S/m**
2,3	-6.11	-5.07	-1.04	1.66×10^{-19}	25.3×10^{-17}
3,4	-6.10	-4.29	-1.81	2.89×10^{-19}	31.1×10^{-30}
4,5	-5.88	-4.42	-1.46	2.33×10^{-19}	19.8×10^{-24}

Zigzag

Adsorption of PLA on center of zigzag CNTs

CNTs /PLA	**E_{HOMO}/eV**	**E_{LUMO}/ eV**	**$\Delta E = E_{HOMO} - E_{LUMO}$ eV**	**$\Delta E = E_{HOMO} - E_{LUMO}$ J**	**$\sigma = e^{-\Delta E/2kT}$ S/m**
4,0	-5.68	-5.42	-0.26	4.165×10^{-20}	39.7×10^{-4}
5,0	-5.60	-4.92	-0.68	1.089×10^{-19}	31.21×10^{-11}

4.4 Mechanical properties of CNT/PLA composite

Mechanical properties determine a material behavior when subjected to mechanical stresses. Among these properties young modulus is measure of solid's stiffness or resistance to elastic deformation , it can be defined as ratio between stress and strain[44].

Young modulus = $\frac{stress}{strain}$

Stress = F/A

Strain = $\frac{l}{\Delta l}$

Where l = original length

P= atmospheric pressure and its value is 101325pa

$\Delta l = Change\ in\ length$

Young modulus = $\frac{F/A}{\Delta l/l}$

Young modulus = $\frac{F}{A} \times \frac{l}{\Delta l}$

As F=PA, so

Y= $\frac{L}{\Delta l} \times P$ …… (1)

From equation number-1, it's clear that young modulus depends upon change in length of material, smaller the change in length of material greater will be young modulus and more will be stiffness.

Mechanical properties of composite are significantly influenced by interfacial interaction between nanotube and polymer matrix, which is critical for improving and manufacturing nanocomposite.[45] [46]

For an armchair CNT having dimensions of (2, 2) (3, 3) (4, 4) (5, 5) with length of 999.2, 986.8, 985.6 and 978.5pm respectively. When PLA is adsorbed on the central surface of CNT

the change in length is observed as 992.7, 985.6, 983.9, and 977.1 pm with young modulus of 2.883×10^7

, 8.332×10^7, 5.874×10^7 and 7.081×10^7 Pa. The lowest change in length is observed for (3, 3) CNT/PLA composite with young modulus of 8.332×10^7 Pa among arm chair CNT.

Two CNTs are selected from chiral CNT having dimensions of (3, 4), (4, 5) for the adsorption of PLA on its surface to investigate its young modulus.it is seen that lowest decrease in length is observed for (4, 5) CNT. The length between C-30 and C-2 is 981.9pm before adsorption but after adsorption its length is 982.8 with young modulus of 9.949×10^8 Pa.

For zigzag CNTs, three CNT having dimensions of (3, 0), (4, 0), (5, 0) are chosen for the adsorption of PLA on its surface. Before adsorption the length of these CNT are 837.6 pm (C-10 to C-27), 837.5 pm (C34-C6), 993.9 pm (C49-C18) respectively, but after adsorption their lengths are changed into 834.0, 822.9, 975.3 pm. Lowest decrease in length is observed for (3, 0) CNT having young modulus of 2.357×10^7 Pa.

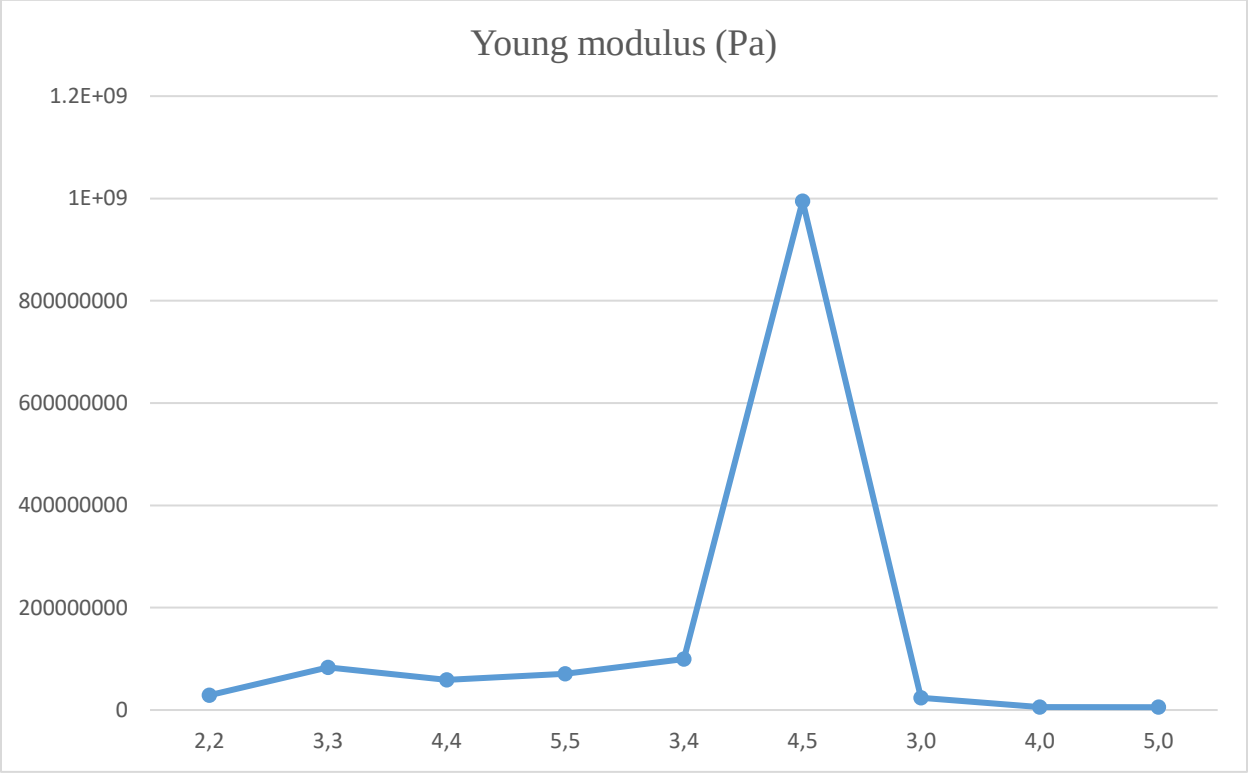

.Above graph showing the highest young modulus for 4, 5 CNT/PLA composite, because PLA transfers its electronic clouds on surface of 4, 5 of CNT and enhanced its matrix density.

Table 4.10 Change in length of CNTs lengths and increase in young modulus upon PLA adsorption

Arm chair

Adsorption of PLA on center of armchair CNTs

CNTs /PLA	**Length of CNTs(pm)**	**CNT/PLA composite**	**Length of CNT/PLA composite (pm)**	**Change in length (Δl)=L-L"**	**Y= $\frac{L}{\Delta l)} \times P$ Pascal**
2,2	996.2	2,2/PLA	992.7	3.5	2.883×10^7
3,3	986.8	3,3/PLA	985.6	1.2	8.332×10^7
4,4	985.6	4,4/PLA	983.9	1.7	5.874×10^7
5,5	978.5	5,5/PLA	977.1	1.4	7.081×10^7

Armchair

Adsorption of PLA on edges of armchair CNTs

CNTs /PLA	**Length of CNTs(pm)**	**CNT/PLA composite**	**Length of CNT/PLA composite (pm)**	**Change in length (Δl)=L-L"**	**Y= $\frac{L}{\Delta l)} \times P$ Pascal**
3,3	986.8	3,3/PLA	984.4	2.4	4.166×10^7
4,4	985.6	4,4/PLA	982.2	3.4	2.937×10^7
5,5	978.5	5,5/PLA	977.6	0.9	1.101×10^8

Table 4.11 Change in length of CNTs lengths and increase in young modulus upon PLA adsorption

Chiral

Adsorption of PLA on center of surface of Chiral CNTs

CNTs /PLA	**Length of CNTs(pm)**	**CNT/PLA composite**	**Length of CNT/PLA composite (pm)**	**Change in length (Δl)=L-L"**	**Y= $\frac{L}{\Delta l}$ × P Pascal**
3,4	985.2	3,4/PLA	984.2	1	9.982×10^7
4,5	981.9	4,5/PLA	981.8	0.1	9.949×10^8

Zigzag

Adsorption of PLA on edges surface of zigzag CNTs

CNTs /PLA	**Length of CNTs(pm)**	**CNT/PLA composite**	**Length of CNT/PLA composite (pm)**	**Change in length (Δl)=L-L"**	**Y= $\frac{L}{\Delta l}$ × P Pascal**
3,0	837.6	3,0/PLA	834.0	3.6	2.357×10^7
4,0	837.5	4,0/PLA	822.9	14.6	5.812×10^6
5,0	993.9	5,0/PLA	975.3	18.4	5.473×10^6

Chapter 5

Conclusion and future perspective

5 Conclusion and future perspective

5.1 Conclusion

Adsorption behavior of PLA on the surface of ten CNTs having different dimensions, is investigated using Density Function Theory (DFT). Electronic, kinetic, thermodynamic and mechanical parameters were calculated for deeper insight into enhancement of CNTs properties. Electronic parameter included E_{HOMO}, $E_{LUMO,}$ ΔE and electrical conductivity are calculated. Highest electrical conductivity is observed for 4, 0 /PLA composite having value of $39.7 \times 10^{-4} Sm^{-1}$ because it have lowest energy gap (-0.26eV) among ten CNTs

Thermodynamic parameter included entropy change, enthalpy change, heat capacity at constant volume and adsorption energy complexation .These parameters determined spontaneity of PLA conjugate formation on CNTs surface and hence stability of complex. The highest value of adsorption constant Kd is calculated for 4,4 CNT/PLA composite having value of $2.74 \times 10^{20} M^{-1}$,this value showing the greater stability of 4,4 CNT/PLA composite.

To find the effect of PLA on mechanical properties of CNTs, young modulus was evaluated based on variation in length of CNTs after PLA adsorption. PLA is adsorbed on the surface of CNTs and decrease in length is observed for each CNT. The highest young modulus is observed for 4, 5 CNT/PLA composite with value of 9.949×10^{8} Pa.

Designing of new composite of CNTs showing remarkable properties *i.e.,* enhanced electrical conductivity, mechanical properties and stability will provide wider applications in mechanical and electronics industry.

5.2 Future Perspective

Carbon nano tube is playing very vital role in mechanical and electronics industries because of its good electrical conductivity and young modulus. Adsorption of PLA enhanced its characteristic so in future metallic wires can be replace by CNT/PLA composite where more efficient conductivity is required *i.e.,* electronic chips, sensor devices ,biomedical machine and in heavy mechanical industries to lift massive load.

6 References:

(1) Zhang, M.; Li, J. Carbon Nanotube in Different Shapes. *Mater. Today* **2009**, *12* (6), 12–18. https://doi.org/10.1016/S1369-7021(09)70176-2.

(2) Golnabi, H. Carbon Nanotube Research Developments in Terms of Published Papers and Patents, Synthesis and Production. *Sci. Iran.* **2012**, *19* (6), 2012–2022. https://doi.org/10.1016/j.scient.2012.10.036.

(3) Coiffic, J. C.; Fayolle, M.; Maitrejean, S.; Foa Torres, L. E. F.; Le Poche, H. Conduction Regime in Innovative Carbon Nanotube via Interconnect Architectures. *Appl. Phys. Lett.* **2007**, *91* (25). https://doi.org/10.1063/1.2826274.

(4) Baughman, R. H.; Zakhidov, A. A.; De Heer, W. A. Carbon Nanotubes - The Route toward Applications. *Science (80-.).* **2002**, *297* (5582), 787–792. https://doi.org/10.1126/science.1060928.

(5) Mat Desa, M. S. Z.; Hassan, A.; Arsad, A.; Mohammad, N. N. B. Mechanical Properties of Poly(Lactic Acid)/ Multiwalled Carbon Nanotubes Nanocomposites. *Mater. Res. Innov.* **2014**, *18*, S6-14-S6-17. https://doi.org/10.1179/1432891714Z.000000000924.

(6) Baei, M. T.; Rastegar, S. F.; Ahmadi Peyghan, A. Surface Modification of Carbon Nanotubes with Nitrenes: A DFT Study. *Fullerenes Nanotub. Carbon Nanostructures* **2015**, *23* (4), 326–331. https://doi.org/10.1080/1536383X.2013.801836.

(7) Williamson, A.; Rajagopal, G.; Needs, R.; Fraser, L.; Foulkes, W. Elimination of Coulomb Finite-Size Effects in Quantum Many-Body Simulations. *Phys. Rev. B - Condens. Matter Mater. Phys.* **1997**, *55* (8), R4851–R4854. https://doi.org/10.1103/PhysRevB.55.R4851.

(8) Skountzos, E. N.; Mermigkis, P. G.; Mavrantzas, V. G. Molecular Dynamics Study of an Atactic Poly(Methyl Methacrylate)-Carbon Nanotube Nanocomposite. *J. Phys. Chem. B* **2018**, *122* (38), 9007–9021. https://doi.org/10.1021/acs.jpcb.8b06631.

(9) Zheng, J.; Zhang, Q.; He, X.; Gao, M.; Ma, X.; Li, G. Nanocomposites of Carbon Nanotube (CNTs)/CuO with High Sensitivity to Organic Volatiles at Room

Temperature. *Procedia Eng.* **2012**, *36*, 235–245. https://doi.org/10.1016/j.proeng.2012.03.036.

(10) Del Canto, E.; Flavin, K.; Natali, M.; Perova, T.; Giordani, S. Functionalization of Single-Walled Carbon Nanotubes with Optically Switchable Spiropyrans. *Carbon N. Y.* **2010**, *48* (10), 2815–2824. https://doi.org/10.1016/j.carbon.2010.04.012.

(11) Moniruzzaman, M.; Winey, K. I. Polymer Nanocomposites Containing Carbon Nanotubes. *Macromolecules* **2006**, *39* (16), 5194–5205. https://doi.org/10.1021/ma060733p.

(12) Dyke, C. A.; Tour, J. M. Overcoming the Insolubility of Carbon Nanotubes Through High Degrees of Sidewall Functionalization. *Chem. - A Eur. J.* **2004**, *10* (4), 812–817. https://doi.org/10.1002/chem.200305534.

(13) Abro, K. A.; Memon, A. A.; Abro, S. H.; Khan, I.; Tlili, I. Enhancement of Heat Transfer Rate of Solar Energy via Rotating Jeffrey Nanofluids Using Caputo–Fabrizio Fractional Operator: An Application to Solar Energy. *Energy Reports* **2019**, *5*, 41–49. https://doi.org/10.1016/j.egyr.2018.09.009.

(14) Andriotis, A. N.; Menon, M.; Srivastava, D.; Chernozatonskii, L. Ballistic Switching and Rectification in Single Wall Carbon Nanotube Y Junctions. *Appl. Phys. Lett.* **2001**, *79* (2), 266–268. https://doi.org/10.1063/1.1385194.

(15) Saifuddin, A. R.; Juniazah, N. Carbon Nanotube: A Review on Structure and Their Interaction. *J. Chem.* **2013**, *2013*, 1–18.

(16) Ballesteros, B.; Torre, G. De; Ehli, C.; Rahman, G. M. A.; Agullo, F.; Guldi, D. M. Single-Wall Carbon Nanotubes Bearing Covalently Linked Phthalocyanines - Photoinduced Electron Transfer. **2015**, No. c, 5061–5068. https://doi.org/10.1021/ja068240n.

(17) Goldoni, A.; Larciprete, R.; Petaccia, L.; Lizzit, S. Single-Wall Carbon Nanotube Interaction with Gases: Sample Contaminants and Environmental Monitoring. *J. Am. Chem. Soc.* **2003**, *125* (37), 11329–11333. https://doi.org/10.1021/ja034898e.

(18) de Jonge, V. N. Feature Article. *Ocean Coast. Manag.* **2013**, *80*, 132.

https://doi.org/10.1016/j.ocecoaman.2013.03.010.

(19) Cheng, Y. C.; Greany, T. Guest Editorial. *Int. J. Educ. Manag.* **2016**, *30* (7), 1166–1170. https://doi.org/10.1108/IJEM-03-2016-0050.

(20) Novais, R. M.; Simon, F.; Pötschke, P.; Villmow, T.; Covas, J. A.; Paiva, M. C. Poly(Lactic Acid) Composites with Poly(Lactic Acid)-Modified Carbon Nanotubes. *J. Polym. Sci. Part A Polym. Chem.* **2013**, *51* (17), 3740–3750. https://doi.org/10.1002/pola.26778.

(21) Garlotta, D. A Literature Review of Poly(Lactic Acid). *J. Polym. Environ.* **2001**, *9* (2), 63–84. https://doi.org/10.1023/A:1020200822435.

(22) Mehta, R.; Kumar, V.; Bhunia, H.; Upadhyay, S. N. Synthesis of Poly(Lactic Acid): A Review. *J. Macromol. Sci. - Polym. Rev.* **2005**, *45* (4), 325–349. https://doi.org/10.1080/15321790500304148.

(23) Jacobsen, S. <Plastcising Pla Jacobsen and Fritz 1999.Pdf>. **1999**, No. 7, 1303–1310.

(24) Zhang, D.; Kandadai, M. A.; Cech, J.; Roth, S.; Curran, S. A. Poly(L-Lactide) (PLLA)/Multiwalled Carbon Nanotube (MWCNT) Composite: Characterization and Biocompatibility Evaluation. *J. Phys. Chem. B* **2006**, *110* (26), 12910–12915. https://doi.org/10.1021/jp061628k.

(25) Lim, J. W.; Hassan, A.; Rahmat, A. R.; Wahit, M. U. Morphology, Thermal and Mechanical Behavior of Polypropylene Nanocomposites Toughened with Poly(Ethylene-Co-Octene). *Polym. Int.* **2006**, *55* (2), 204–215. https://doi.org/10.1002/pi.1942.

(26) Gao, Y.; Song, G.; Adronov, A.; Li, H. Functionalization of Single-Walled Carbon Nanotubes with Poly(Methyl Methacrylate) by Emulsion Polymerization. *J. Phys. Chem. C* **2010**, *114* (39), 16242–16249. https://doi.org/10.1021/jp104894a.

(27) Misak, H. E.; Asmatulu, R.; Omalley, M.; Jurak, E.; Mall, S. Functionalization of Carbon Nanotube Yarn by Acid Treatment. *Int. J. Smart Nano Mater.* **2014**, *5* (1), 34–43. https://doi.org/10.1080/19475411.2014.896426.

(28) Lepak-Kuc, S.; Podsiadły, B.; Skalski, A.; Janczak, D.; Jakubowska, M.; Lekawa-Raus, A. Highly Conductive Carbon Nanotube-Thermoplastic Polyurethane Nanocomposite for Smart Clothing Applications and Beyond. *Nanomaterials* **2019**, *9* (9). https://doi.org/10.3390/nano9091287.

(29) Rinderspacher, B. C. An Introduction to Theoretical Chemistry. By Jack Simons. *Angew. Chemie Int. Ed.* **2004**, *43* (8), 923–924. https://doi.org/10.1002/anie.200385028.

(30) Perdew, J. P.; Burke, K.; Ernzerhof, M. Generalized Gradient Approximation Made Simple. *Phys. Rev. Lett.* **1996**, *77* (18), 3865–3868. https://doi.org/10.1103/PhysRevLett.77.3865.

(31) Guardiola, R. Monte Carlo Methods in Quantum Many-Body Theories. *Microsc. Quantum Many-Body Theor. Their Appl.* **2008**, 269–336. https://doi.org/10.1007/bfb0104529.

(32) Van Mourik, T.; Gdanitz, R. J. Heory StudiA Critical Note on Density Functional Tes on Rare-Gas Dimers. *J. Chem. Phys.* **2002**, *116* (22), 9620–9623. https://doi.org/10.1063/1.1476010.

(33) Kohn, W.; Becke, A. D.; Parr, R. G. Density Functional Theory of Electronic Structure. *J. Phys. Chem.* **1996**, *100* (31), 12974–12980. https://doi.org/10.1021/jp960669l.

(34) Burke, K. Perspective on Density Functional Theory. *J. Chem. Phys.* **2012**, *136* (15). https://doi.org/10.1063/1.4704546.

(35) Becke, A. D. Perspective: Fifty Years of Density-Functional Theory in Chemical Physics. *J. Chem. Phys.* **2014**, *140* (18). https://doi.org/10.1063/1.4869598.

(36) Segall, M. D.; Lindan, P. J. D.; Probert, M. J.; Pickard, C. J.; Hasnip, P. J.; Clark, S. J.; Payne, M. C. First-Principles Simulation: Ideas, Illustrations and the CASTEP Code. *J. Phys. Condens. Matter* **2002**, *14* (11), 2717–2744. https://doi.org/10.1088/0953-8984/14/11/301.

(37) Alrawashdeh, A. I.; Lagowski, J. B. The Role of the Solvent and the Size of the

Nanotube in the Non-Covalent Dispersion of Carbon Nanotubes with Short Organic Oligomers-a DFT Study. *RSC Adv.* **2018**, *8* (53), 30520–30529. https://doi.org/10.1039/c8ra02460j.

(38) Alaghemandi, M.; Müller-Plathe, F.; Bhm, M. C. Thermal Conductivity of Carbon Nanotube-Polyamide-6,6 Nanocomposites: Reverse Non-Equilibrium Molecular Dynamics Simulations. *J. Chem. Phys.* **2011**, *135* (18). https://doi.org/10.1063/1.3660348.

(39) Frankland, S. J. V.; Harik, V. M.; Odegard, G. M.; Brenner, D. W.; Gates, T. S. The Stress-Strain Behavior of Polymer-Nanotube Composites from Molecular Dynamics Simulation. *Compos. Sci. Technol.* **2003**, *63* (11), 1655–1661. https://doi.org/10.1016/S0266-3538(03)00059-9.

(40) Mera-Adasme, R.; Mendizábal, F.; Olea-Azar, C.; Miranda-Rojas, S.; Fuentealba, P. A Computationally Efficient and Reliable Bond Order Measure. *J. Phys. Chem. A* **2011**, *115* (17), 4397–4405. https://doi.org/10.1021/jp107498h.

(41) Smith, D. G. A.; Patkowski, K. Toward an Accurate Description of Methane Physisorption on Carbon Nanotubes. *J. Phys. Chem. C* **2014**, *118* (1), 544–550. https://doi.org/10.1021/jp410826p.

(42) Zhao, Y.; Truhlar, D. G. The M06 Suite of Density Functionals for Main Group Thermochemistry, Thermochemical Kinetics, Noncovalent Interactions, Excited States, and Transition Elements: Two New Functionals and Systematic Testing of Four M06-Class Functionals and 12 Other Functionals. *Theor. Chem. Acc.* **2008**, *120* (1–3), 215–241. https://doi.org/10.1007/s00214-007-0310-x.

(43) Geng, J.; Kinloch, I. A.; Singh, C.; Golovko, V. B.; Johnson, B. F. G.; Shaffer, M. S. P.; Li, Y.; Windle, A. H. Production of Carbon Nanofibers in High Yields Using a Sodium Chloride Support. *J. Phys. Chem. B* **2005**, *109* (35), 16665–16670. https://doi.org/10.1021/jp051544w.

(44) Frankland, S. J. V.; Caglar, A.; Brenner, D. W.; Griebel, M. Molecular Simulation of the Influence of Chemical Cross-Links on the Shear Strength of Carbon Nanotube-

Polymer Interfaces. *J. Phys. Chem. B* **2002**, *106* (12), 3046–3048. https://doi.org/10.1021/jp015591+.

(45) Woldemariam, M. H.; Belingardi, G.; Koricho, E. G.; Reda, D. T. Effects of Nanomaterials and Particles on Mechanical Properties and Fracture Toughness of Composite Materials: A Short Review. *AIMS Mater. Sci.* **2019**, *6* (6), 1191–1212. https://doi.org/10.3934/MATERSCI.2019.6.1191.

(46) Guo, D.; Xie, G.; Luo, J. Mechanical Properties of Nanoparticles: Basics and Applications. *J. Phys. D. Appl. Phys.* **2014**, *47* (1). https://doi.org/10.1088/0022-3727/47/1/013001.